Analytical and HYDRUS2D Modeling for Buried Peat-filled Trapezoidal Ditches as Subsurface Capillarity-Driven Irrigating Units: the Kornev-Vedernikov 2-D Seepage Revisited

Anvar Kacimov[1], *Yurii Obnosov*[2,5], *Tatyana Nikonenkova*[3], *Andrey Smagin*[4,5]

[1]Department of Soils, Water and Agricultural Engineering, Sultan Qaboos University, Oman

[2]Institute of Mathematics and Mechanics, Kazan Federal University, Kazan, Russia

Emails: anvar@squ.edu.om; akacimov@gmail.com

ORCID ID: orcid.org/0000-0003-2543-3219

[2]Institute of Mathematics and Mechanics, Kazan Federal University, Kazan, Russia

Emails: yobnosov@kpfu.ru; yurii.obnosov@gmail.com

ORCID ID: orcid.org/0000-0001-9220-7989

[3]Institute of Ecology and Geography, Kazan Federal University, Kazan, Russia

Email: nikonentv@gmail.com

ORCID ID 0000-0002-8871-216

[4]Department of Soil Physics and Melioration, Faculty of Soil Sciences, Lomonosov Moscow State University, Moscow, 119991 Russia

[5]Institute of Forest Science, Russian Academy of Sciences, Uspenskoe, 143030 Russia

Email: avsmag1965@gmail.com

ORCID ID: orcid.org/0000-0002-3483-3372

Short title for running head: Capillarity-Driven Seepage

Submitted to Modeling Earth Systems and Environment (Springer),

https://link.springer.com/journal/40808

Address for correspondence:

Prof. Kacimov A.R.,

Department of Soils, Water and Agricultural Engineering

Sultan Qaboos University Al-Khod 123, PO Box 34 Sultanate of Oman

Tel (968) 24141-3668 Fax (968) 24413-418

Emails: anvar@squ.edu.om

akacimov@gmail.com

Omani page:

https://www.squ.edu.om/agr/Departments/Soils-Water-and-Agricultural-Engineering/Faculties/Prof-Anvar-Kacimov

Abstract

Two mathematical models, an analytical and numerical, describe 2D Darcian seepage of in subsurface irrigation from a ditch, with pore moisture sucked up and laterally from a non-standard "emitter", which is engineered as a channel of a small depth with a lined (impervious bottom). For steady flow in a homogeneous, saturated, rigid, isotropic porous medium a boundary value problems to Laplace's equation for characteristic functions of the piezometric head and stream function is solved by the method of hodograph, i.e. conformal mapping of two polygons in complex plains onto each other via a reference plane. For a transient saturated-unsaturated seepage from th ditch or a buried permeable pipe in this ditch, initial boundary value problems (IBVPs) to the Richards equation are numerically solved using HYDRUS2D package. Both models give the vector fields of specific discharge (Darcian velocity) and scalar fields of pressure head, volumetric moisture content, isotachs, as well as flow nets. Applications of the models are to design and construction of urban and agricultural soils ("constructozems"), as porous composites, with the aim at optimizing the soil moisture consumption by the plants by minimizing evaporation and deep percolation. For this purpose a lens (or double-periodic cluster of lenses) made of peat or other relatively coarse material is buried under the ground surface. This lens(es) is surrounded by a fine-textured indigenous soil. The pore water motion to/from the lens, acting intermittently as a draining entity (collecting pore water from the ambient soil) and a subsurface irrigator (emitting water to this soil), in such an engineered smartly-heterogenized vadose zone becomes essentially 2-D. Our models substantiate the field experiments by Kornev (1935) who backfilled ditches and generated capillarity-maintained "wet bulbs" in the root zone. We also complete Vedernikov's (1940) analytical solution for steady 2-D seepage from a trapezoidal ditch having a zero-depth water level.

Keywords: subsurface capillarity-driven irrigation, complex potential and hodograph domains, conformal mappings, HYDRUS2D modeling.

1. Introduction

Mathematical modeling of steady-state Darcian seepage of an incompressible fluid (pore water in our case) in homogeneous, saturated, rigid isotropic porous media involves solving boundary value problems (BVP) to Laplace's equation, with respect to the piezometric head (see e.g. Strack, 1989). If the medium is anisotropic, a more general elliptic partial differential equation (PDE) models flows in soils (see e.g. Polubarinova-Kochina, 1962, hereafter abbreviated as PK-62). In these models, the capillarity of soil is ignored that is correct for flow in dams' foundations and confined aquifers. For steady flows through earth dams and in unconfined aquifers a phreatic surface (free boundary) emerges, with a capillary fringe and the vadose zone above it that requires solving BVPs to parabolic PDEs. In transient saturated-unsaturated flows, initial boundary value problems (IBVPs) have to be solved, with the Richards equation describing variations of the pressure head, volumetric moisture content, fluxes and other flow parameters (see e.g. Radcliffe and Šimůnek 2018, Namaghi et al., 2015). In applications to geotechnical engineering (e.g. in design of earth dams), analytical and numerical methods (AaNM), as well as sandbox physical modeling experiments are used (see e.g. Cedergren, 1989, Fawzy et al., 2024). In this paper, we apply AaNM, *viz.* the theory of holomorphic functions (PK-62, Strack, 1989) and finite element method, realized in the software HYDRUS2D (Šimůnek et al. 2016) to model seepage flows from buried subsurface emitters placed under row crops.

In subsurface irrigation, most common technique of water supply is through perforated plastic pipes placed at the depth of several cm-tens of cm, in the root zone of plants, with mathematical models for seepage from such type of sources (see e.g. Lamm et al., 2007). Kornev (1921, 1935, hereafter abbreviated as K-35) and Vedernikov (1939, 1940, abbreviated as V-40), correspondingly, worked on irrigation projects, which involved furrows (surface irrigation) and uncommon subsurface emitters. The work in K-35 and V-40 was not completed in the sense of both engineering realization and modeling. We engage the modern modeling tools of AaNM, *viz.* computer algebra (Wolfram's, 1991, *Mathematica*) and HYDRUS2D, to advance the Kornev-Vedernikov experimental-analytical legacy and make it user-friendly for irrigation engineers.

K-35 developed two original systems of subsurface irrigation (SI, see e.g. Goyal, 2014 for a recent review of this method of microirrigation) of crops' root zones in semi-arid and arid regions of France and the USSR. Moisture was sucked from buried horizontal, systematic "line 2D sources" (the terminology of Strack, 1989) by the ambient natural dry soil and transpirative uptake by crops' roots. The source of "sub-root zone" water was:

A) Unglazed clay-made pipes, where water was under negative pressure (tension). Mathematical models of seepage from these systematic buried emitters were developed by PK-62 and Strack (1989).

B) Ditches, backfilled to a certain depth by a coarse ("imported") porous medium, which was capped at the top by the "natural" fine-textured soil.

In this paper, we focus on K-35 system B). An elementary cell of a periodic system, a rectangle $M_1M_2M_3M_4$, is depicted in Fig.1 (a vertical cross-section perpendicular to the ditch axis).

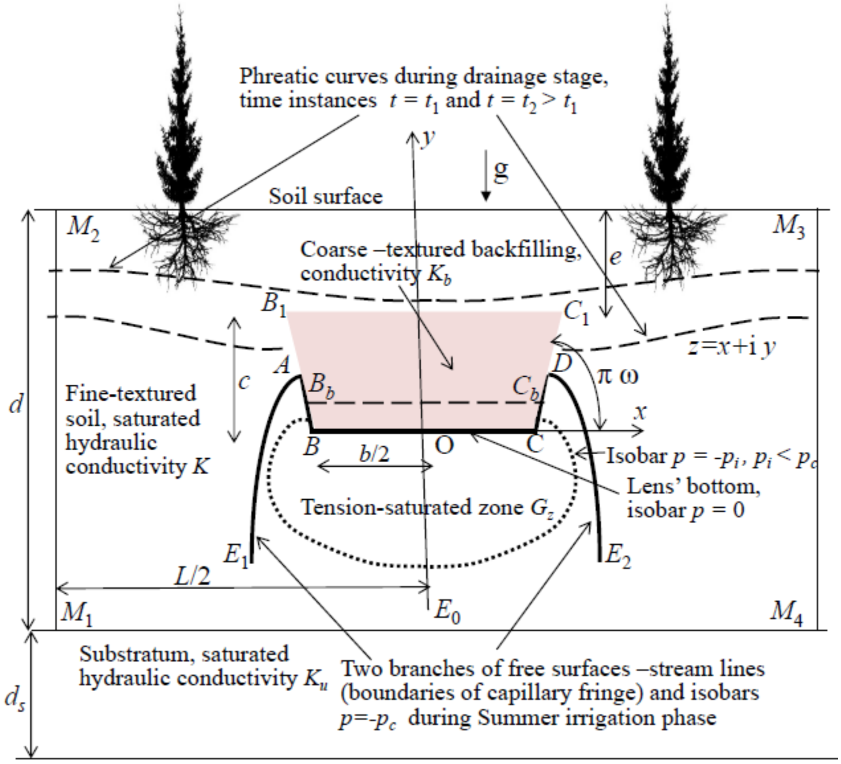

Fig.1 Vertical cross-section of seepage domain for K-35 trapezoidal ditch.

A lens BB_1C_1C in Fig.1 is filled with peat, fascines, sand or other highly permeable medium. The lens is trapezoidal with the angle of bank slope $\omega\pi$, $0 < \omega < 1/2$, the bottom width b and height c. The depth of burial, e, is counted from a horizontal soil surface M_2M_3 to B_1C_1 (the "cap" of the backfilling). Such engineered soil composites are successfully used as "constructozems" (Bakhmetova et al., 2022) in arid irrigated agriculture, desert afforestation, and urban landscaping. The technology increases the topsoil water retention and protects it from secondary salinization. Peat or synthetic gel-forming polymer super-absorbents can be also used as backfilling.

High total water capacity (up to 90-95 vol. % for peat and up to 60-70 vol.% for 0.1-0.3 mass% mixtures of gels with soil) and "field capacity" (40-60% at pressure heads of –100 kPa) guarantee reliable retention of irrigation water when introducing 1-2 parallel lenses of these artificial materials into the topsoil (see e.g. Arkhangelskaya, 2024). The pore water accumulation of layered soil composites is enhanced by the effect of capillary barriers, the physical phenomenon widely used in geotechnical engineering (see e.g. Radclif and Šimůnek, 2010, Feng et al., 2025). Field tests of layered constructozems confirmed a reduction (by 40–70%) in unproductive water losses to deep percolation and evaporation. The productive water consumption by plants increased up to 70–130%, the total volume of irrigation water dropped by 20–50%. The dry aboveground (photosynthetic) biomass increased up to 1.7–2.5 times, and the belowground root phytomass increased up to 1.5–2 times in tested fresh crop yields (see e.g. Deeb et al., 2024). Separation of the topsoils from subsoils by a capillary barrier made of coarse-textured materials or water repellents reliably protects the root zone from secondary salinization by interrupting the capillary rise of water-soluble salts from saline groundwater and deep highly salinized soil strata. During unexpected catastrophic downpours, as, for example, in the United Arab Emirates and Oman in April 2024, the coarse-textured subsoil screen acts as a drainage system.

So far, design of constructozems used numerical modeling (HYDRUS-1D package) of 1-D water and solutes transport and root water consumption in the "soil-plant-material" system. However, the 1D models are applicable only in the case of flat landscapes with plane-parallel lenses of soil modifiers. In the case of a relief with slopes, as well as for local soil constructions (tree and shrub pits, holes for vegetable crops with drip irrigation, etc.), a more complex flow of water with dissolved substances takes place that requires 2,3-D modeling.

In our model, we study an elementary cell of a periodic SI system (Fig.1). The horizontal and vertical sizes of this cell (the flow domain for a saturated-unsaturated seepage) are L and d, respectively. A system of Cartesian coordinates (x,y) has its origin at point O, the middle of the ditch bed BC. The complex physical coordinate is $z = x$ i y. The natural soil profile may have a substratum of thickness d_s.

After the Spring snowmelt (in crop fields with hydromorphic soils of Russia, see e.g. Kovalev, 2019), rare torrential Summer rains and/or periodic sprinkling from above in the hyperarid climate of Arabia, the lens works as a drain. The progressive and rapid drawdown of the phreatic curve is illustrated in Fig.1 for two time instances: t_1 and t_2. During hot and dry seasons (few weeks in Russia and permanently in the Gulf countries), the lens acts as a moisture emitter for the “natural” soil. Therefore, the more pore water is stored in the lens and the more is uptaken by the root zone in the finer soil, the better. In other words, the infiltrated water, which was stored during the drainage phase, is “absorbed” (K-35 terminology) by a desiccated soil during the irrigation phase. Also, if the infiltrated pore water storage in the coarser component of the composite is insufficient, then a systemic supply to the lens from a tank placed on the ground surface is set up (see K-35 for details).

We consider the case of the triad of hydraulic conductivities of the composite (lens-soil-substratum in Fig.1), which obey the double inequality $K_b > K > K_u$. We model seepage during a dry Summer season in K-35 such that the water level above BOC in Fig.1 is maintained low, aiming at reducing deep percolation and increasing water use efficiency. Irrigation of the root-containing zone is controlled by seepage from the horizontal segment BOC (a zero-pressure isobar).

Flow is determined by gravity, Darcian resistance of the composite porous matrix and capillarity of the fine-textured soil (Lamm et al., 2007).

The analytical and numerical models give the following:

- the seepage flow rate per unit length of the lens Q [m^2/s in SI],
- isobars p = const (p is the pressure head [m]),
- the position of the curves AE_1 and DE_2 (along these streamlines $p = -p_c$ = const), which cap the capillary fringe (CF),
- the flow net,
- isotachs $|\vec{V}|$ = const , where $\vec{V}$ is the vector of Darcian velocity ([m/s]),
- isohumes,
- isochrones t = const for marked pore water particles,
- time-variation of flow characteristics at selected observational points,

among others.

2. Methods

2.1Analytical Model

In this subsection, we follow V-40 and engage the hodograph method (see PK-62, Samal and Mishra, 2017, 2022, Strack, 1989, Bakker and Post, 2022) to analyze the steady-state, tension-saturated, 2-D seepage in a homogeneous flow domain, G_z, laterally sandwiched between the two branches of free surfaces (CF boundaries). Muromtsev (1991) reported on intricate subzoning of CFs but in our model we neglect such hairsplitting. Thus, CF in Fig.1 is capped from above by an equipotential horizontal segment of the ditch bed and two slanted segments of the ditch slopes (streamlines). In the analytical model, we assume that the size L (Fig.1) is large enough such that the free surfaces AE_1 and BE_2 generated by the K-35 neighbouring irrigation ditches do not intersect with each other.

The Darcy law states $\vec{V}(x,y) = -K\nabla h$ where $h(x,y) = p(x,y)\ \ y$ is the total (piezometric) head and p is the pressure head. The velocity potential, $\varphi = -K\ h$, a stream function is ψ and a complex potential is $w = \varphi + \mathrm{i}\psi$. A complex Darcian velocity is $V = u\ \ \mathrm{i}v$, where $u(x,y)$ and $v(x,y)$ are the horizontal and vertical components of $\vec{V}$.

During hot and dry Summers, water is channeled (see K-35) perpendicular to the plane of Fig.1. Positive values of p in the ditch and in the adjacent "natural" soil is maintained by a finite water depth flowing to the ditch from a positive-pressure surface tank. A certain slope in the direction perpendicular to the plane of Fig.1 (e.g. the topographic slope in Manning's formula) may be needed if the ditch is long. In our analytical model, a zero-depth ponding of the interface between a coarse filling of the trapezium and the subjacent fine-textured soil makes the whole domain G_z tension saturated. We recall that seepage from a non-buried Riesenkampf's zero-depth channel (PK-62, Section 6, Chapter 5) was also purely tension-saturated. Point O in Fig.1 is fiducial such that along BOC $\varphi = p = 0$, while, owing to symmetry, $\psi = 0$ along OE_0. According to the Vedernikov-Bouwer model, the branches E_1A and E_2D of the CF boundary are streamlines along which $\psi = \mp Q/2$, $p = -p_c$, where p_c [m] is the height of capillary rise of the soil (see PK-62, and Vedernikov, 1939 for tabulated values of this constant for various soils. For sandy soils and peat, for example, PK-62, her Table 5, p.19 reports p_c=100-150 cm for sandy soils and 120-150 cm for peat).

Strictly speaking, for a composite dyad of fine and coarse soils in Fig.1, there is a mild vertical capillary rise in the backfilling. A horizontal segment B_bC_b (Fig.1, dashed line) "caps" a tension-saturated zone (CF) inside the peat filling of the trapezium. In our analytical model, we ignore seepage in this coarse backfilling.

The complex potential domain G_w is a half-strip shown in Fig.2a (zigzagged blue lines here and in other Figures indicate the interior of the domains in complex plains). We assume that the substratum M_1M_4 is deep enough such that points E_1, E_2 and E_0 collapse into a single point E, the infinity on the Riemann sphere. Therefore, in the vernacular of Strack (1989) a generalized dipole is made by a source of a finite length b, placed at $y = 0$, and a sink at infinity ($y \to -\infty$).

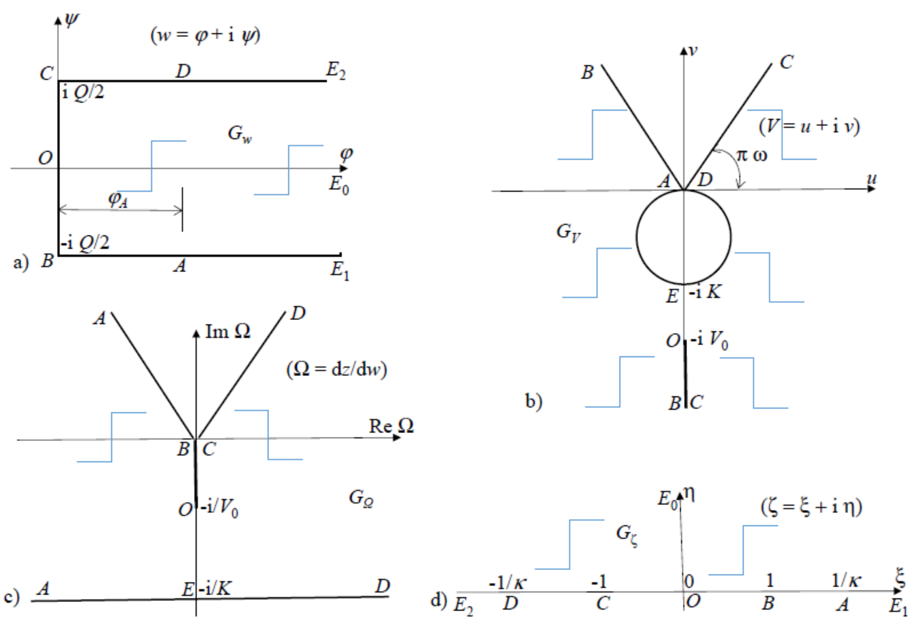

Fig.2 Complex potential domain (a), hodograph domain (b), inverted hodograph domain (c), reference half-plane (d).

The finite-length segments *BA* and *CD* on the banks of the trapezium are streamlines along which the pressure head drops from 0 to $-p_c$. A dotted curve in Fig.1 exemplifies an "intermediate" isobar sandwiched between *BOC* and free boundaries. A dashed curve in Fig.1 is a streamline which starts at the horizontal bottom of the ditch (sufficiently close to point *C*). Along this flow path a water particle moves, first, vertically down (gravity prevails), after that it moves up (capillarity prevails) and, finally, descends vertically down again (gravity again takes over capillarity).

The potential φ_A at points *A* and *D* is a part of solution. The whole G_z is tension-saturated, i.e. $-p_c < p(x,y) < 0$ there.

The hodograph domain, G_V, corresponding to G_z, is depicted in Fig.2b. This domain is a circular pentagon bounded by two rays *DC* and *AB*, a circle *AED* of a radius *K*, centered at the point $V = -\mathrm{i}\, K/2$ and a semi-infinite vertical cut *BOC* with its tip at the point $V = -\mathrm{i}\, V_0$, where V_0 (a part of solution) is the magnitude of Darcian velocity at point *O*. Velocity at points *A* and *D* is zero and at points *B* and *C* is infinite. Our G_V is a special case of one in V-40 (see Fig.147 in PK-62). We mirror G_V with respect to the axis $v = 0$ in the *V*-plane. That gives a circular pentagon in the plane of a holomorphic function $\mathrm{d}w/\mathrm{d}z = u - \mathrm{i}v$. After that, we use the method of inversion (see PK-62, Section 5, Ch. 5) and get the polygon G_Ω shown in Fig.2c, where $\Omega = \mathrm{d}z/\mathrm{d}w$ is another holomorphic function.

PK-62 (pp.160-162) reported the V-40 solution to a more general problem for a finite depth of water inside the trapezium. V-40 obtained his solution and presented results in an inverse manner, *viz.* he specified two conformal mapping (so-called "accessory") parameters. Next, he evaluated the geometrical sizes of the channel and the depth of water in it. After 1950, Vedernikov could not complete the analysis which he started in V-40. We use a direct method, i.e. specify the physical (including geometrical) parameters and find an unknown conformal mapping (accessory) parameter. As compared with the epoch of V-40 and even Aravin and Numerov (1953), PK-62, we have computer algebra (Wolfram's, 1991, *Mathematica*, Python, MatLab, etc.) arsenals to solve a nonlinear equation with respect to this parameter. We also operate HYDRUS2D for modeling geometries and soil compositions more general than one in V-40.

Thus, we apply the Schwarz-Christoffel formula to map G_w and G_Ω onto the upper half-plane G_ζ of the reference plane $\zeta = \xi + \mathrm{i}\eta$ (Fig.2d) with the correspondence of points $O \to 0, B \to 1, C \to -1, A \to 1/\kappa, D \to -1/\kappa, E \to \infty$, where $0 < \kappa < 1$ is a mapping parameter. The corresponding mapping functions are:

$$w = -\mathrm{i}\frac{Q}{\pi}\arcsin\zeta\,, \tag{1}$$

$$\Omega(\zeta) = \frac{\mathrm{d}z}{\mathrm{d}w} = \mathrm{i}R\int_0^{\zeta}\tau(1-\tau^2)^{\omega-1/2}(1-\kappa^2\tau^2)^{-\omega-1}\mathrm{d}\tau - \frac{\mathrm{i}}{V_0} =$$

$$= \frac{\mathrm{i}R/2}{\omega(1-\kappa^2)}\left(f(0) - (1-\zeta^2)^{\omega+1/2}(1-\kappa^2\zeta^2)^{-\omega} f(\zeta)\right) - \frac{\mathrm{i}}{V_0}\,, \tag{2}$$

where

$$f(\zeta) = \mathrm{F}\left(\frac{1}{2}, 1; 1-\omega; \frac{1-\kappa^2\zeta^2}{1-\kappa^2}\right) =$$
$$-2\omega\frac{1-\kappa^2}{1-\kappa^2\zeta^2}\mathrm{F}\left(1, 1+\omega; \frac{3}{2}; \frac{1-\kappa^2}{1-\kappa^2\zeta^2}\right) - \mathrm{i}\frac{\sqrt{\pi}}{k^{1+2\omega}}\sqrt{\frac{1-\kappa^2}{1-\zeta^2}}\frac{\Gamma(1-\omega)}{\Gamma(1/2-\omega)}\left(\frac{1-\kappa^2\zeta^2}{1-\zeta^2}\right)^{\omega} \tag{3}$$

and

$$f(0) = -\sqrt{1-k^2}\left(2\omega\sqrt{1-k^2}\,\mathrm{F}\left(1, 1+\omega; 3/2; 1-\kappa^2\right) + \mathrm{i}\frac{\sqrt{\pi}\,\Gamma(1-\omega)}{k^{1+2\omega}\Gamma(1/2-\omega)}\right) \tag{4}$$

Here F stands for the hypergeometric function ${}_2\mathrm{F}_1$ and Γ for the gamma function (Abramowitz and Stegun, 1968). All multivalued complex functions above are fixed in the upper half-plane to be positive at $0 < \xi < 1$ (see Henrici, 1993 for more details).

The positive constant *R*, found from the condition $\Omega(1) = 0$, is

$$R = \frac{(1+2\omega)}{V_0\,\mathrm{F}(1, 1+\omega; 3/2+\omega; \kappa^2)}\,. \tag{5}$$

At point *E* seepage is unidirectional, with a unit hydraulic gradient, i.e. we consider the regime without “backwater” (the vernacular of PK-62); a more general condition at infinity, with “backwater” (zero velocity at infinity) can be analyzed as in PK-62. From eqns. (2), (3) and the no “backwater” condition $\Omega(\mathrm{i}\infty) = -\mathrm{i}/K$ we get

$$\int_0^{\mathrm{i}\infty}\tau\frac{(1-\tau^2)^{\omega-1/2}}{(1-\kappa^2\tau^2)^{\omega+1}}\mathrm{d}\tau = -\int_0^{\infty}\tau\frac{(1+\tau^2)^{\omega-1/2}}{(1+\kappa^2\tau^2)^{\omega+1}}\mathrm{d}\tau = \frac{\mathrm{F}\left(1, 1+\omega; 3/2+\omega; \kappa^2\right)}{1+2\omega} - \frac{\sqrt{\pi}\,\Gamma(1/2+\omega)}{2\kappa^{2\omega+1}\sqrt{1-\kappa^2}\,\Gamma(1+\omega)}\,. \tag{6}$$

Then, from eqns. (2), (4) follows

$$\left(\frac{1}{K}-\frac{1}{V_0}\right)\mathrm{F}\left(1,1+\omega;3/2+\omega;\kappa^2\right)=\frac{1+2\omega}{V_0}\left(\frac{\sqrt{\pi}\,\Gamma(1/2+\omega)}{2\kappa^{2\omega+1}\sqrt{1-\kappa^2}\,\Gamma(1+\omega)}-\frac{\mathrm{F}\left(1,1+\omega;3/2+\omega;\kappa^2\right)}{1+2\omega}\right) \tag{7}$$

wherefrom

$$V_0=K\frac{(1+2\omega)\sqrt{\pi}\,\Gamma(1/2+\omega)}{2\kappa^{2\omega+1}\sqrt{1-\kappa^2}\,\Gamma(1+\omega)\,\mathrm{F}\left(1,1+\omega;3/2+\omega;\kappa^2\right)}\ . \tag{8}$$

Eqn.(1) at point *A* gives

$$\varphi_A=\operatorname{Re} w(1/\kappa)=\frac{Q}{\pi}\operatorname{Im}\left(\arcsin\frac{1}{\kappa}\right)=\frac{Q}{\pi}\operatorname{arccosh}\frac{1}{\kappa}. \tag{9}$$

By the help of eqns. (1), (2) we find

$$z(\zeta)=\frac{Q}{\pi}\left(\left(\frac{R}{2\omega(1-\kappa^2)}f(0)-\frac{1}{V_O}\right)\arcsin\zeta-\frac{R}{2\omega(1-\kappa^2)}\int_0^{\zeta}\left(\frac{1-\tau^2}{1-\kappa^2\tau^2}\right)^{\omega}f(\tau)\mathrm{d}\tau\right), \tag{10}$$

where R and V_0 are expressed in eqns. (5) and (8) respectively.

From eqn.(10), according to Fig.1a, follows $z(-1)=b/2$. Using the last condition, equation (3) and the resulting representation for $f(0)$, it can be shown that

$$Q=bV_0\Bigg/\left(1+\frac{1+2\omega}{\mathrm{F}(1,1+\omega;3/2+\omega;\kappa^2)}\left[f_1(0)-\frac{2}{\pi}\int_{-1}^{0}\frac{\left(1-\tau^2\right)^{\omega}}{\left(1-\kappa^2\tau^2\right)^{\omega+1}}f_1(\tau)\mathrm{d}\tau\right]\right)\ , \tag{11}$$

where

$$f_1(\tau)=\mathrm{F}\left(1,1+\omega;\frac{3}{2};\frac{1-\kappa^2}{1-\kappa^2\tau^2}\right). \tag{12}$$

The equality $\varphi_A/K+y_A=p_c$ (the CF condition in the Vedernikov-Bouwer model, PK-62, which is – up to notations – equivalent to the Green-Ampt 1-D infiltration model), where φ_A is defined by eqn.(9), and $y_A=\operatorname{Im} z(1/\kappa)=\operatorname{Im} z(-1/\kappa)$, results in a nonlinear equation with respect to κ:

$$\left(\frac{1}{K}-\frac{1}{V_0}-R\,\mathrm{F}(1,1+\omega;3/2;1-\kappa^2)\right)\operatorname{arcosh}\frac{1}{\kappa}+\frac{R\,\mathrm{Sin}\,\pi\omega}{2\omega(1-\kappa^2)}\int_1^{1/\kappa}\left(\frac{\tau^2-1}{1-\kappa^2\tau^2}\right)^{\omega}f(\tau)\mathrm{d}\tau=\frac{\pi p_c}{Q}. \tag{13}$$

In eqn. (13), the values of *R*, V_0, and *Q* are determined via eqns. (5), (8) and (11), respectively. We used the routine **FindRoot** of Wolfram’s (1991) *Mathematica* for solving eqn.(13).

2.2 HYDRUS model

Due to the symmetry of the flow domain (Fig.1) we consider its right half only. The Richards PDE is solved in HYDRUS package (see e.g. Radcliffe and Šimůnek, 2018 for more details) with respect to $p(x,z,t)$ by the method of finite elements. In subsection 2.1, seepage was steady state and, therefore, the Vedernikov-Bouwer model reduces Richards' PDE to the Laplace PDE, for which BVPs are solved by various methods of the theory of holomorphic functions (Aravin and Numerov, 1953, PK-62, Strack,1989). In subsection 2.2, we deal with transient seepage (time, t, is an independent physical variable), in which the analogues of analytical free surfaces are asymptotically attained by moving boundaries (Crank, 1984). Consequently, initial boundary value problems (IBVP) are solved by HYDRUS2D (no analytical solutions are available for these IBVPs).

3. Results

In the analytical model we introduce dimensionless quantities: $(z^*, w^*, V^*, R^*, Q^*, b^*) = (z/p_c, w/(K p_c), V/K, R*K, Q/(K p_c), b/p_c)$ and – for the sake of brevity - drop the superscript "*". We used the routines **Re** and **Im** of *Mathematica* and in Fig.3 plotted the flow nets (see Cedergren, 1989 for the details related to these nets) for $b = 1$, $\omega = 0.1$ and 0.5, panels (a) and (b), respectively. The lower panel (c) in Fig.3 zooms one streamline ($\psi = 1.7$, $\omega = 0.5$), which starts at the bottom of the ditch, close to its corner (point C in Fig.1). This streamline has a local minimum and global maximum, i.e. has a non-trivial shape, if compared with "standard" streamlines for seepage from soil channels without capillarity (PK-62). The intricacy of the form of the streamlines, which start on OC and are adjacent to point C, geometrically demonstrate the interaction of three physical seepage-controlling factors, *viz.* gravity, Darcian resistance of the porous skeleton and capillarity.

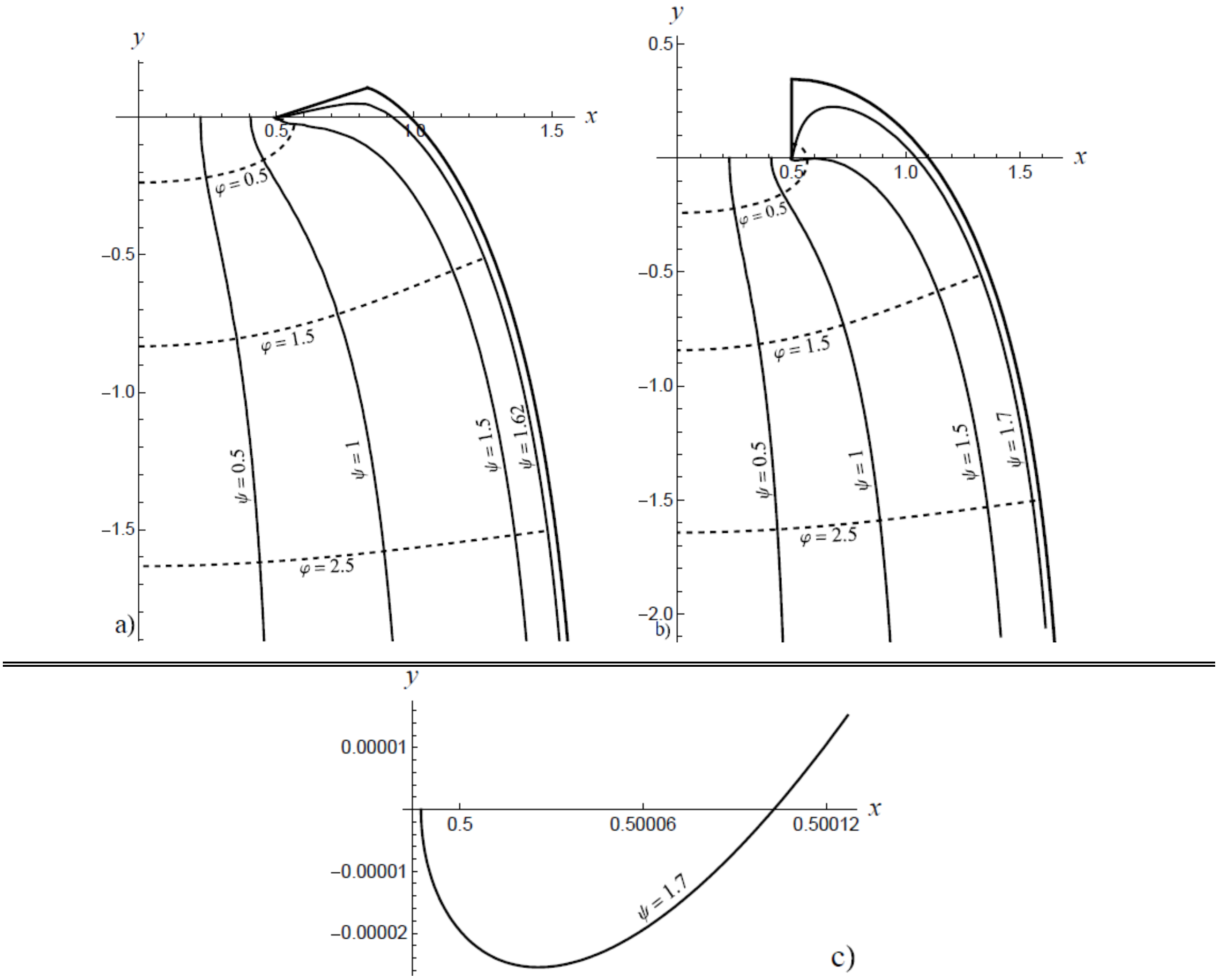

Fig.3. Flow net for b = 1, ω = 0.1 (a) and ω = 0.5 (b), zoomed non-trivial streamline with a local minimum near the ditch bed (c).

In Table 1 the accessory parameter κ, seepage flow rate Q and minimal velocity magnitude along the trapezium bed V_0 for several ditch slopes are computed for b =1.

ω	0.001	0.1	0.2	0.3	0.4	0.5
κ	0.66079	0.722784	0.767840	0.801263	0.826804	0.846834
$Q(\omega,\kappa)$	3.22055	3.298939	3.357662	3.402614	3.437979	3.466441
$V_0(\omega,\kappa)$	2.17890	2.168398	2.158476	2.149812	2.142405	2.136100

Table 1. Accessory parameter κ, flow rate Q and minimal velocity magnitude V_0 (along the trapezium bed) for several ditch slopes (b =1).

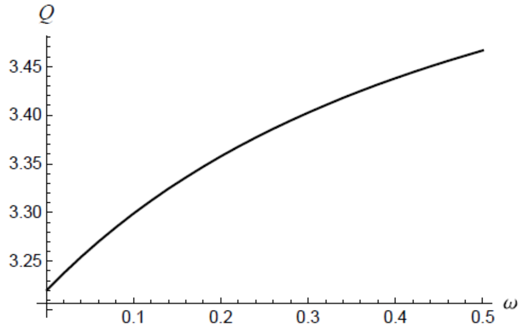

Fig.4. Seepage flow rate as a function of ω the V-40 trapezium slope (b =1).

In Fig.4, the function $Q(\omega)$ is plotted for b = 1. Riesenkampf's solution (see PK-62, pp. 162-166) for ω = 0 yields (in modern notations) the following nonlinear equation with respect to Q:

$$\frac{2Q\exp[-\pi/Q]}{\pi^2}\Phi[\exp[-2\pi/Q],2,1/2]=b, \quad (14)$$

where $\Phi[z,s,a]$ is the Lerch transcendent (**LerchiPhi** in a *Mathematica* routine, Wolfram, 1991). For the case of b = 1 in Figs.3-4 and Table 1, eqn. (14), solved by the **FindRoot** routine of *Mathematica*, gives Q = 3.21962 that is less than only 0.05% less than the corresponding value for ω = 0.001. Overall, in the whole range of practical values of the trapezium slope, its impact on Q is minor, i.e. the Riesenkampf solution- in comport with the comparison theorems (Goldstein and Entov, 1994) - gives not only a lower bound of Q for any trapezium of a given b, but even a very good approximation for any ω. Most wadis in the Gulf (see e.g. Sen, 2008) are ephemeral or intermittent streams, *viz.* they do not flow or flow with a small water depth (except of course, the rare and short flashflood events) and, therefore, the slope of their banks is not important if the value of Q is of concern.

For the sake of brevity, we drop the results of analytical computations for other values of b.

In the numerical model, which works with dimensional quantities, we selected several Kornev's subsurface irrigation designs. In HYDRUS, computer programs with models of specific flow patterns are called "Projects" and the vertical coordinate is z.

Project 1. Without any loss of generality we select the V-40 trapezium, having $\pi\omega$ = arctan(2/15). Other geometrical parameters of the elementary cell are: $l_v = l_h$ = 300 cm, b = 50 cm, e = 20 cm, b_1 =200 cm (Fig.5, left panel). Therefore, physically the distance between the axes of Kornev's ditches (periodic-systematic SI of row crops, like maize in K-35) is 600 cm. The soil is the Van Genuchent (VG) sand (see the HYDRUS soil catalogue), for which the VG hydraulic parameters are K = 712.8 cm/day, α = 0.145 1/cm and n = 2.68. The FE mesh discretization parameters were: 14212 nodes, 27906 triangular 2D and 528 1D elements.

Our IBVP, which geometrically and in the asymptotic limit $t \to \infty$ is close to one in subsection 2.1. We used the initial condition, which is default in HYDRUS, *viz.* $p(x,z,0)$ = -100 cm that corresponds to an almost irreducible volumetric moisture content θ_r = 0.045 of the VG sand. The origin of HYDRUS Cartesian coordinates (xOz) is now at the midpoint of the trapezium bed such that the soil surface is at the horizon z = 100 cm and the free drainage horizon is at z = -200

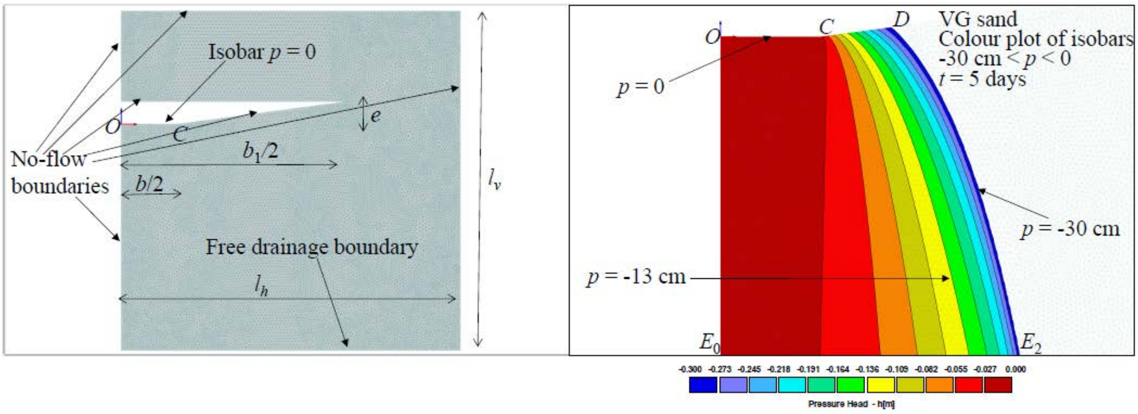

cm.

Fig.5. HYDRUS2D geometry, FE nodes, boundary conditions (left panel); isobars in Project 1 (right panel).

The boundary conditions for the HYDRUS octagon in Fig.5 are: no flow everywhere, except the outlet free drainage horizon (z = -200 cm) and the zero-pressure inlet OC (a segment of a width $b/2$=50 cm), i.e. we have a simple flow tube. Physically, the condition at OC means that the water level in the buried ditch is zero but water is continuously injected into the ditch from an external tank, as K-35 did in his irrigated crop fields. Therefore, the V-40 and K-35 problems are mathematically matched in terms of boundary conditions. We also note that evaporation from the soil surface and transpiration by the plants' roots are ignored.

The total HYDRUS simulation time is 5 days, although steady state seepage is attained in half a day. The right panel in Fig.5 demonstrates the palette of isobars, plotted in the range -30 cm < p < 0 for t = 5 days. The isobars p = 0, -13 cm and -30 cm are arrowed. The analytical and numerical solutions can be matched by comparing the free boundary $p = -p_c$ in subsection 2.1 with one of the isobars in Fig.5. Obviously, none of the HYDRUS isobars is a streamline, contrary to the analytical solution where the CF boundary (free surface) is. In Fig.6, we plotted the HYDRUS isotachs (left panel) and the vector-field of Darcian velocity. Fig.6 demonstrates that high velocities are concentrated near the trapezium corner C, where the hydraulic gradients are almost 2 that exceeds the PK-62 limit of 1 at which porous media are stable in the sense of suffusion and other types of seepage-induced instability. Therefore, the bed of our HYDRUS trapezium is a line of potential lessivage for the subjacent ambient soil.

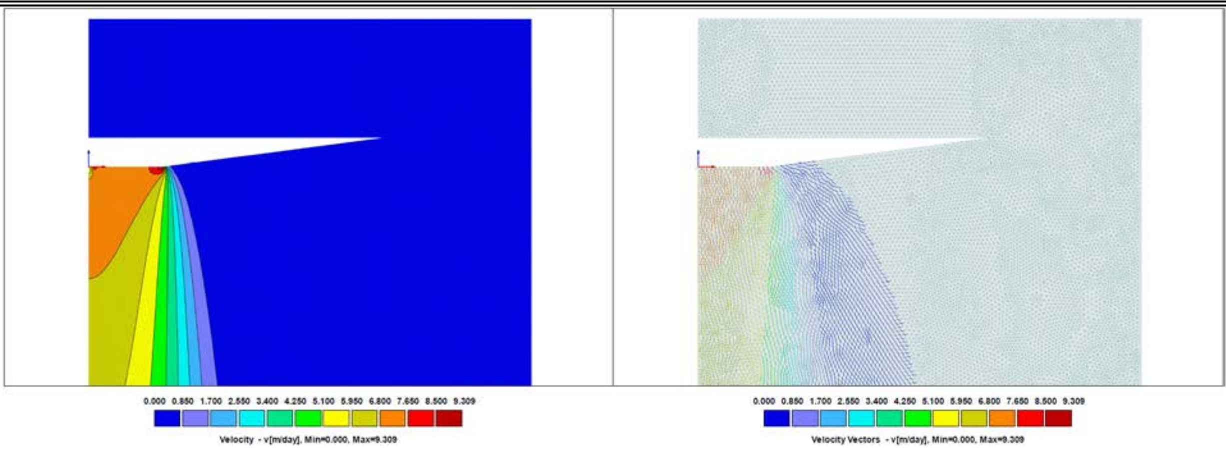

Fig.6. Isotachs and Darcian velocities in HYDRUS Project 1.

The HYDRUS dimensional, almost steady-state flow rate for the seepage domain in Fig.5 is $Q_H = 3.93 * 10^4$ cm^2/day.

For the sake of brevity, we skip over the sensitivity analysis, in which we truncated-expanded (from the right and beneath) the flow domain in Fig.5, refined the FE mesh, changed the initial conditions for *p*, and varied the VG constants (α, n, k).

<u>Project 2.</u> Now we consider a saturated-unsaturated seepage from a circular emitter having the diameter of 10 cm. K-35 placed such positive-pressure pipes at the bottom of ditches. The width and height of our rectangular ditch are 40 cm and 25 cm, correspondingly (Fig.7, left panel). The soil surface is 45 cm above the ditch bed. The HYDRUS flow rectangle is 100 cm wide and 245 cm tall. The ambient soil is the VG loam (see the HYDRUS soil catalogue), which is characterized by (α, n, K) = (0.036 1/cm, 1.56, 25 cm/day). The VG parameters for our peat are: K_u = 480 cm/day, α = 0.0381/day, n = 1.216, θ_s = 0.916, θ_r = 0.02. These parameters are consistent with ones reported by Boelter et al. (1977) and were experimentally obtained in our lab for the backfilling of the lenses, earlier modeled in HYDRUS-1D only. The lenses were designed and constructed as experimental constructozems for blue spruce seedlings (*Picea pungens* Engelm.) in the Serebryanoborsky forest, The Forestry Institute, the Russian Academy of Sciences, Moscow.

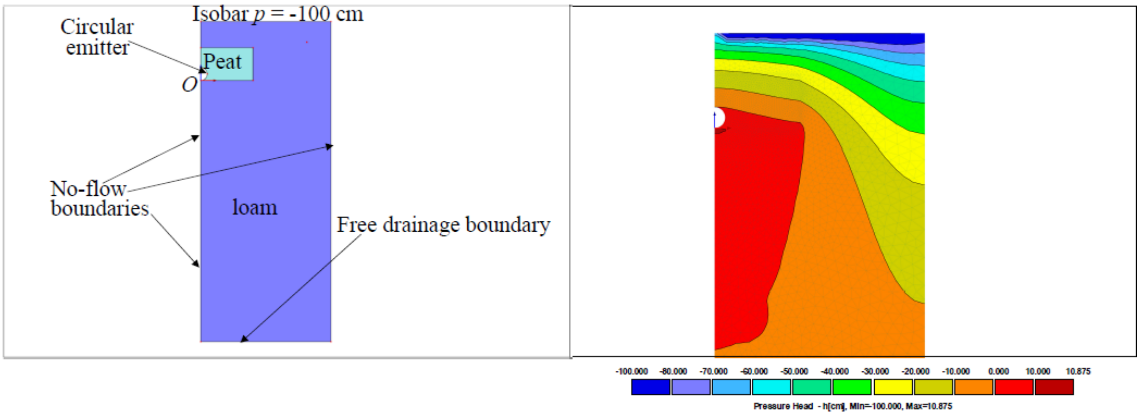

Fig.7. HYDRUS Project 2 flow domain with a perforated pipe emitting water into a peat-filled rectangular ditch embedded into an ambient loam (left panel) and isobars at t = 60 days (right panel).

The topsoil boundary condition is now p = -100 cm, i.e. a pretty high dryness of the loam is imposed on the soil surface. The mesh is coarser than in Project 1 but is refined near the emitting semi-circle, along which the boundary condition is a hydrostatic pressure distribution with p=0 at the apex of the semi-circle and p = 10 cm at its lowest point. Thus, the flow domain is not a simple flow tube as in Project 1 above.

Isobars for t = 60 days (almost steady-state seepage) are shown in Fig.7, right panel.

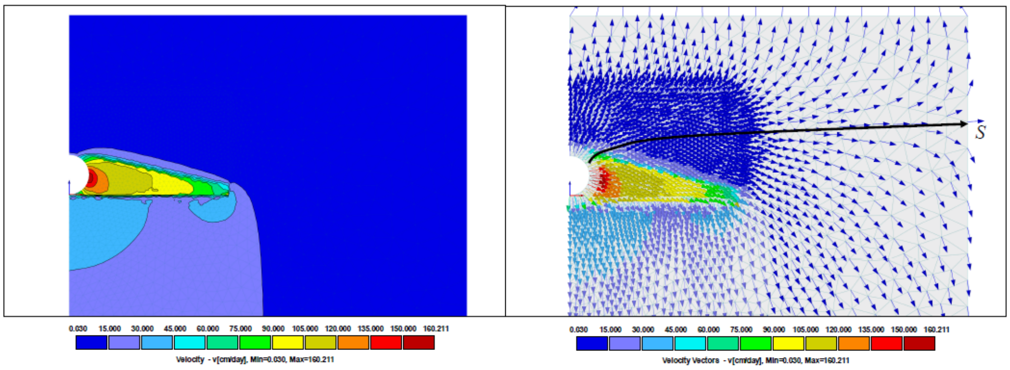

Fig.8. HYDRUS isotachs (left panel) and velocity vectors at t = 60 days (right panel) in the vicinity of K-35 ditch.

At t = 60 days, a snapshot of isotachs and of the vector field of the Darcian velocity is shown in Fig.8. A separatrix (only schematically sketched) is depicted as an arrowed streamline with a stagnation point S at the right boundary of the HYDRUS flow domain. This streamline is a watershed boundary between what seeps from the emitter to the atmosphere and what descends to deep percolation.

We also modeled a three-component composite soil with a VG clay substratum (for the sake of brevity we do not add the corresponding HYDRUS-generated Figures). Specifically, we modified the flow domain in Fig.7 (left panel) by adding a VG clay layer having d_s = 10 cm (see Fig.1) and the pentad of VG hydraulic parameters K_u = 0.1 cm/day, α = 0.008 1/day, n = 1.09, θ_s = 0.38, θ_r = 0.068. The flow topology drastically changed, as compared with what is depicted in Figs. 7-8. Specifically, the abscissa of the stagnation point S decreased from z_s = 15 cm (Fig.8 left panel) to z_s = -69 cm. The “inverted” (the terminology of Sophocleous, 2002) water table p = 0 which “hangs” under the K-35 in Fig.7 (right panel) is transformed into a “normal” (almost horizontal) water table. In other words, the deep clay layer (Fig.1) makes soil under emitter fully saturated with an almost linear (in z) increase of positive p within the loam stratum. The deep drainage flow rate decreases to 8.67 cm^2/day as compared with 1500 cm^2/day in Project 2. All these results warn: the soil heterogeneity (even trivial layering) and seepage conditions at infinity, deep under the soil surface are very important (see e.g. Philip et al., 1989) if simulation times are long (“seasonal” - “annual” – “decadal” – “centennial” – “millennial”), rather than short (a single “irrigation” or “rainfall” event).

4. Conclusions

Steady, 2D seepage from a trapezoidal channel into a capillary soil, in which the tension-saturated zone and CF are modeled by the Vedernikov-Bouwer approximation of the soil hydraulic conductivity. The modern tools of computer algebra made possible solution of a nonlinear equation with respect to the accessory parameter in a conformal mapping, reconstruction of the flow net, determination of the seepage flow rate as a function of the slope of the V-40 trapezium. Our analytical solution for an arbitrary slope of the trapezium matches well the Riesenkampf one for zero-depth channels.

In HYDRUS2D modeling, which is versatile in demonstrating how the unsaturated soils uptake moisture from a buried, subirrigation source and spread it up and laterally, against gravity. Our analytical and HYDRUS simulations showed how the seepage flow rate from a non-trivial subsurface source (a backfilled ditch with an impermeable bed as a barrier to deep percolation) depends on the width of the ditch, slope of the bank and hydraulic properties of the soil or soil composite through which moisture is spread from the buried K-35 emitter. We also plotted the palettes and contours of isobars, isohumes, isotachs, and flow nets which demonstrate the efficiency of the K-35 subsurface irrigation method. Of special interest are the “free boundaries” in the analytical model, viz. the water table or the “cap” of CF. They are plotted and compared with ones compute by HYDRUS.

On behalf of all authors, the corresponding author states that there is no conflict of interest.

Acknowledgements

This work was funded by SQU, grants IG/AGR/SWAE/22/02, IG/VC/WRC/21/01, DR/RG/17 and by Russian Scientific Foundation, interdisciplinary project no. 23-64-10002. Valuable comments by an anonymous referee are appreciated.

References

Abramowitz M, and Stegun IA (1968) Handbook of Mathematical Functions With Formulas, Graphs, and Mathematical Tables (Vol. 55). US Government printing office, Washington

Aravin VI, Numerov SN (1953) Theory of Fluid Flow in Undeformable Porous Media. Gostekhizdat, Moscow (in Russian). English Translation: Israel Program for Scientific Translation, Jerusalem, 1965.

Arkhangelskaya TA, Telyatnikova EV, Umarova AB (2024) Thermal diffusivity of soil-peat mixtures: nonlinear dependence on peat Content. Moscow University Soil Science Bulletin, 79(4), 478-484.

Bakhmatova KA, Matynyan NN, Sheshukova AA (2022) Anthropogenic soils of urban parks: A review. Eurasian Soil Science, 55(1), 64-80.

Bakker M, Post V (2022) Analytical Groundwater Modeling: Theory and Applications Using Python. CRC, Boca Raton.

Boelter DH, Verry ES (1977) Peatland and water in the northern lake states (No. 31). USDA Forest Service, North Central Forest Experiment Station.

Cedergren HR (1989) Seepage, Drainage and Flow Nets. Wiley, New York.

Crank J (1984) Free and Moving Boundary Problems. Clarendon Press, Oxford.

Deeb M, Smagin AV, Pauleit S, Fouch´e-Grobla O, Podwojewski P, Groffman PM (2024) The urgency of building soils for Middle Eastern and North African countries: Economic, environmental, and health solutions. Science of the Total Environment, 917, 170529. https://doi.org/10.1016/j.scitotenv.2024.170529

Fawzy MA, Hassan NA, Saad NY, El-Molla DA (2024). Experimental and numerical modeling of diaphragm grouting in earth dams considering construction defects. Modeling Earth Systems and Environment, 10(2), 2159-2185.

Feng S, Zheng Y, Liu H, Li G, Qian X (2025) Numerical study of rainfall percolation through a novel capillary barrier cover with a zipper-shape interface between fine-and coarse-grained soils. Waste Management, 191, 220-229.

Goldstein R, Entov V (1994) Qualitative Methods in Continuum Mechanics. Chapman and Hall, New York.

Goyal MR (ed.) (2014) Sustainable Practices in Surface and Subsurface Micro Irrigation. Apple Academic Press, New York.

Henrici P (1993) Applied and Computational Complex Analysis. Volume 3: Discrete Fourier Analysis, Cauchy Integrals, Construction of Conformal Maps, Univalent Functions. Wiley. New York.

Kornev VG (1921) Method and device for subsurface irrigation using pipes. USSR patent N 139. Корнев В.Г., 1921. Способ и устройство для подпочвенного орошения с применением труб. Патент СССР, N 139.

Kornev VG (1935) Subsoil Irrigation (absorption irrigation method). Moscow, Selkhozgiz (in Russian). Корнев В.Г., 1935. Подпочвенное орошение (метод абсорбционного орошения). Москва, Сельхозгиз.

Kovalev IV (2019) Transformation of semi-hydromorphic soils drained with plastic and pottery drainage. In the collection "*Soil reclamation for sustainable development of agriculture*", 30-38. Materials of the International Scientific and Practical Conference, Kirov, Vyatka State Agricultural Academy (in Russian). Ковалев, И.В., 2019. Трансформация полугидроморфных почв, осушенных пластмассовым и гончароным дренажом. В сборнике «Мелиорация почв для устойчивого развития сельского хозяйства», 30-38. Материалы Международной научно-практической конференции, Киров, Вятская Государственная Сельскохозяйственная Академия.

Lamm FR, Ayars JE, Nakayama FS (eds.) (2023). Microirrigation for Crop Production: Design, Operation, and Management. Elsevier, Amsterdam.

Muromtsev NA (1991) Soil Hydrophysics for the Purpose of Reclamation. Leningrad, Gidrometeoizdat (in Russian). Муромцев НА (1991). Мелиоративная гидрофизика почв. Ленинград, Гидрометеоиздат.

Namaghi H, Li S, Jiang L (2015). Numerical simulation of water flow in a large waste rock pile, Haizhou coal mine, China. Modeling Earth Systems and Environment, 1, 1-10.

Philip JR, Knight JH., Waechter RT (1989) Unsaturated seepage and subterranean holes: Conspectus, and exclusion problem for circular cylindrical cavities. Water Resources Research, 25(1),16-28.

Polubarinova-Kochina PYa (1962) Theory of Ground Water Movement. Princeton University Press, Princeton. Second edition of the book in Russian is published in 1977, Nauka, Moscow.

Radcliffe DE, Šimůnek J (2018) Soil Physics With HYDRUS: Modeling and Applications. CRC, Boca Raton.

Robinson NI (2023) New analysis and numerical values for the classical dam problem. Advances in Water Resources, 175, p.104356.

Samal KP, Mishra GC (2017) Analysis of seepage from a triangular furrow considering soil capillarity using inverse hodograph and conformal mapping technique. ISH Journal of Hydraulic Engineering, 23(1), 1-12.

Samal KP, Mishra GC (2022) Analysis of seepage from parallel triangular furrows by inverse hodograph and conformal mapping technique. In Jha et al. (eds.), *"Hydrological Modeling"*, Water Science and Technology Library 109, pp. 459-478 , Springer https://doi.org/10.1007/978-3-030-81358-1_35

Sen, Z. (2008) Wadi Hydrology. CRC, Boca Raton.

Šimůnek J, van Genuchten MTh, Šejna M (2016) Recent developments and applications of the HYDRUS computer software packages, Vadose Zone J., 15(7), doi: 10.2136/vzj2016.04.0033.

Sophocleous M (2002) Interactions between groundwater and surface water: the state of the science. Hydrogeology J., 10, 52-67.

Strack ODL (1989) Groundwater Mechanics. Prentice-Hall, Inc., Englewood Cliffs.

Vedernikov VV (1939) Theory of Seepage and Its Applications to Problems of Irrigation and Drainage, Gosstroiizdat, Moscow (in Russian).

Vedernikov, V. V. (1940). Account of soil capillarity on seepage from a canal, Doklady AN SSSR, 28, (5) (in Russian).

Wang W, Wang X, Zhang A, Liu H., Huang Y (2025). Targeted strategy of straw derived hydrogels for sustainable water and fertilizer. Science of The Total Environment, 959, p.178153.

Wolfram S (1991). *Mathematica*. A System for Doing Mathematics by Computer. Addison-Wesley, Redwood City.

LIST OF ABBREVIATIONS:

1) AaNM= analytical and numerical methods
2) BVP= boundary value problem
3) CF=capillary fringe
4) IBVP= initial boundary value problem
5) K-35=Kornev V.G., 1935. *Subsoil Irrigation (absorption irrigation method)*. Moscow, Selkhozgiz (in Russian)
6) PDE=partial differential equation
7) PK-62= Polubarinova-Kochina, P.Ya., 1962. *Theory of Ground-water Movement.* Princeton University Press, Princeton. Polubarinova-Kochina, P.Ya., 1977. *Theory of Ground-water Movement*. Nauka, Moscow (in Russian)
8) SI= subsurface irrigation
9) V-40= Vedernikov, V. V., 1940. Account of soil capillarity on seepage from a canal, Doklady AN SSSR, 28 (5) (in Russian)
10) VG=Van Gnuchten